APPENDIX 2.

GREENHOUSE GAS FLUX MEASUREMENTS

1. Chamber flux measurements and calculations

This appendix brings together, in summary form, all of the methods used to measure and estimate gas fluxes using chambers at the field sites. The original documents and resources are separately available.

1.1. Chamber design and deployment

Collars used on the project were square in plan view, with sides of 60 cm (3600 cm^2). Onto these could be placed acrylic chambers of varying heights. The chambers had two components: (a) the chamber itself, and (b) stackable sections that could be used to extend the height of the chamber. The latter comprised four walls constructed from 3-mm thick acrylic sheet that was cut to lengths of 600 mm and heights of 500 mm. Each side was bolted and sealed to aluminium angle (Figure 1.1). The chambers were similar to the stackable sections but were shorter with a height of 300 mm and were fitted with an upper acrylic lid welded to the walls (Figure 1.1). The collars were made in a similar way to the stackable sections but from 3-mm polyvinyl chloride (PVC) sheets and not acrylic. Figure 1.1 below shows a near-final prototype of the setup: the collar, sections and chamber can all be seen. Air-tight seals between the components were achieved by using silicone sponge fitted to the top edge of the collar and each stackable section. The lower edge of the unit (stackable section or chamber) above rests on this sponge, providing a seal.

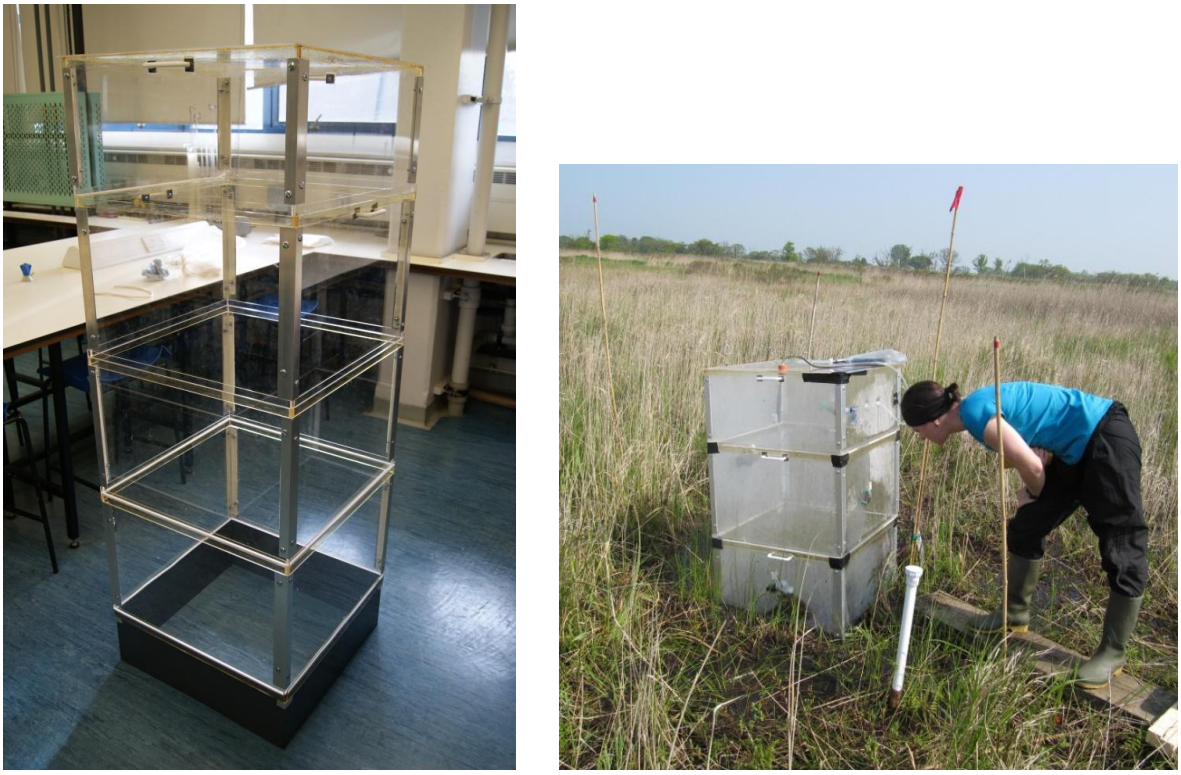

Figure 1.1 *Left: Photograph of collar, flux chamber and three flux chamber extensions. This shows a near-final prototype that is very similar, except in details like the handles, to those that were used across the project. Right: the prototype being used at the NB-LN site.*

Six collars were deployed at each site, with the location of these chosen to reflect the site's target (or dominant) vegetation types (see main report). In tall-stature vegetation, the collars were constructed so that 15 cm of them were below the ground surface and 15 cm above. In short vegetation, shorter collars were used; these extended to the same depth (15 cm), but only 5 cm of the collar was left protruding above the ground surface. Collars were permanently installed at the majority of sites, but it was necessary to remove and reinstall collars at arable sites to avoid damage during agricultural operations; at these sites, collars were re-installed the day before measurements were made. Flux chamber tests were conducted throughout the year to ensure winter flux estimates were properly obtained, but were more frequent in spring and summer when the CH_4 and N_2O fluxes and gross primary productivity and ecosystem respiration (see section 5) are greatest. In each year of the study, tests were conducted, where possible, in the weeks shown in Table 1.1 below.

Table 1.1. *Target week numbers for the flux chamber tests at each site. Non-core sites – TM-EX, TM-W, NB-LN, and NB-HN – had different (lower-frequency or shorter duration) sampling regimes.*

Week 2 (Jan)	**Week 30** (Jul)
Week 7 (Feb)	**Week 32** (Jul/Aug)
Week 11 (Mar)	**Week 34** (Aug)
Week 14 (Apr)	**Week 36** (Sept)
Week 18 (Apr/May)	**Week 39** (Sept)
Week 21 (May)	**Week 42** (Oct)
Week 24 (June)	**Week 46** (Nov)
Week 26 (June)	**Week 51** (Dec)
Week 28 (Jul)	

1.2. Chamber tests and measurement protocols

1.2.1 Background

Flux chamber tests are used to measure fluxes of target gases – in this project CO_2, CH_4, and N_2O – between the soil-vegetation system and the atmosphere above. The principle of a test is simple. Assume, for example, that CH_4 is the target gas and is being emitted from a peatland into the atmosphere above. If a box open at its base is placed on the peatland surface, one would expect to see an increase in CH_4 concentrations within the box over time. The rate of change in CH_4 concentration will be directly proportional to the flux or emission rate. A chamber fitted to a collar is simply a type of box. In practice, flux chamber tests can be quite involved and it is necessary to measure the temperature and pressure of the air contained within the chamber and to take precautions against test-related artefacts that may lead to erroneous gas flux estimates.

To circulate the air within it, each chamber was fitted with a fan (or fans if there were additional stacked sections). Sunon (Kaohsiung City, Taiwan) slim-line axial fans were used. These are normally used to cool the electronic components within computers and have a capacity of 5 m^3 hr^{-1}. One was used per chamber and per stacked section. Therefore, in a chamber extending 1.3 m above a collar, three fans would be needed: one for each stackable section of 500 mm and one for the top chamber section of 300 mm. During tests, measurements were also made of the air temperature and pressure within a chamber. Air pressures within

the chambers were equalised with the external air pressures using a double gas bag arrangement. A tube was fitted across the chamber wall, with each end of the tube fitted to a partially-inflated gas bag. Changes in pressure between the inside and outside of the chamber would be equalised via air flow between the bags. For example, if the pressure outside the chamber rose, the external gas bag would compress and air move from it into the inner gas bag. As the inner gas bag expanded, the pressure of the air within the chamber would increase (in response to the loss of volume caused by the expanding gas bag). Air pressures were measured outside the chamber using a Commeter (Comet Systems, Rožnov pod Radhoštěm, Czech Republic) C4141 meter. The same meter was also used to measure within-chamber temperature. The meter comprised a readout unit which also housed the pressure sensor, and a separate cylindrical probe which contained the temperature sensor. The readout unit remained outside the chamber during a test while the probe was inserted into the chamber. The probe was fitted through a rubber bung which was then plugged into a hole in the chamber lid so that an air-tight seal was formed, with the sensor held within the chamber.

The way in which particular tests were conducted depended on the target gas and the equipment available for measuring the concentration of the gas. The different possibilities are explained in sections 1.2.2-1.2.4 below.

1.2.2 Chamber tests: measuring CO_2 exchanges with an infra-red gas analyser (IRGA)

For measuring CO_2 exchange using an infra-red gas analyser (IRGA) or similar portable device, the following protocol was employed:

a. The pressure-equalisation bags on the chamber (chamber side walls) were inflated to about one third of their capacity.
b. The fan or fans was/were switched on.
c. The gas analyser's inlet and outlet tubes were inserted into the chamber.
d. Leaving the port for the temperature probe open, the chamber or chamber and stackable sections was/were placed on the collar.
e. The Commeter C4141 temperature probe was inserted into the chamber.
f. The time in GMT was noted. This time was important for the modelling work discussed in section 5. For the models it was necessary to match measurements from other instruments such as water-table wells to each chamber test flux estimate.
g. The temperature and pressure from the Commeter C4141 probe and the time in seconds since chamber closure (since insertion of the Commeter probe) were noted.
h. $[CO_2]$ (square brackets denote concentration) was measured in ppmv or ppbv at five evenly-spaced times (i.e., a time series) over a period of between 30s and 150 s since chamber closure.
i. The temperature and pressure from the Commeter C4141 probe and the time in seconds since chamber closure (since insertion of the Commeter probe) were again noted.
j. The chamber was removed from the collar for 60 seconds.
k. The Commeter probe was removed from its port.
l. A reflective shroud was placed over the chamber and any stackable sections.
m. Steps d to i were repeated.
n. The chamber was removed from the collar and its fan(s) switched off.

1.2.3 Chamber tests: measuring CH_4 and N_2O fluxes by taking gas samples and measuring gas concentrations in them in the laboratory

CH_4 or N_2O fluxes may be estimated by taking gas samples from a chamber during a test and then later analysing these samples for their respective gas concentrations in the laboratory. In this case the protocol was as follows:

a. The pressure-equalisation bags on the chamber (chamber side walls) were inflated to about one third of their capacity.
b. The fan or fans was/were switched on.
c. A reflective shroud was placed over the chamber and any stackable sections.
d. Leaving the port for the temperature and humidity probe(s) open, the chamber or chamber and stackable sections was/were placed on the collar.
e. The Commeter C4141 temperature probe was inserted into the chamber.
f. The temperature and pressure from the Commeter C4141 probe and the time in seconds since chamber closure (since insertion of the Commeter probe) were noted.
g. At intervals of 1, 6, 11, 16, and 21 minutes[1] after chamber closure gas samples were removed from the chamber via a septum port in the chamber wall using a syringe fitted with a needle. Samples of gas were stored either in gas-tight (lockable) syringes or in pre-evacuated gas-tight vials (only factory- or rig- evacuated vials were used).
h. The temperature and pressure from the Commeter C4141 probe were again noted 9 minutes and 20 minutes after chamber closure.
i. After the last gas sample was taken the chamber was removed from the collar.

Both CH_4 and N_2O concentrations were measured using gas-chromatography – flame ionisation detector methods (GC-FID) (details not given here).

1.2.4 Chamber tests: measuring CO_2 and CH_4 exchanges simultaneously with a Los Gatos gas analyser

Most of the site teams had access to a new portable instrument manufactured by Los Gatos Research (San Jose, California, USA) called an Ultraportable Gas Analyser (UGA) that measures simultaneously CO_2, CH_4 and H_2O gaseous concentrations. For those teams that had access to a UGA and for sites where N_2O fluxes were very low, it was possible to replace the separate flux chamber tests described above in 1.2.2 and 1.2.3 with a single set of tests. Here the protocol was virtually identical to that in 1.2.2 except that the UGA replaced the IRGA. Also, because the UGA is programmable and can measure gas concentrations at high frequencies (e.g., 1 Hz) it was not necessary to take readings manually at intervals of several seconds. Instead, a test typically lasted for 3-5 minutes and yielded 180-300 readings for each gas species of interest.

1.2.5 Order of tests

The order in which chambers are sampled was noted and varied between trips. For example, if all sampling trips involved a flux test at 09.00 GMT, the collar used for the test would vary between trips. Thus, collar 'xxxx1' may have been used first for a test on trip *a* and last on the next trip, trip *b*. The order of tests was varied such that there was no bias in the time of sampling any particular collar. Such variation was particularly important for the longer tests involving the collection of gas samples (as described above in 1.2.3).

[1] These intervals could be lengthened if fluxes were very low.

1.3. Converting flux test data into flux estimates

As noted above in section 1.2.1, changes in the concentration of any gas within a flux chamber can be used to estimate ecosystem-atmosphere exchanges of that gas. The flux of any gas between the peatland and the atmosphere may be calculated from the following (Denmead, 2008):

$$F_g = \frac{V}{A}\frac{d\rho_g}{dt} \quad (1)$$

where F_g is the gas flux density at the peatland surface (M L^{-2} T^{-1} – mg m^{-2} day^{-1}), V is the combined volume of the flux chamber and the collar above the peatland surface, A is the inside area of the collar (L^2 – m^2), ρ_g is the mass concentration of the gas in the chamber (M L^{-3} – mg m^{-3}), and t is time (T – days).

On SP1210 (and the previous Defra project SP1202) equation (1) was solved in slightly modified form, as:

$$F_g = \frac{1}{A}\frac{dg_m}{dt} \quad (2)$$

where g_m is the mass of the gas in the chamber (M – mg) ($g_m = V \times \rho_g$). A set of calculations was written as a spreadsheet for use by the project's site teams. In outline, these calculations were as follows:

a. Calculate the *volume* of the target gas in the chamber at each time a sample was taken or a measurement made.
b. Convert this volume into an equivalent volume under standard temperature and pressure (STP).
c. Convert the volume under STP into moles of gas.
d. Convert the number of moles of gas into a mass.
e. Fit a linear regression (ordinary least squares) through the mass *vs* time data to give a *rate* of increase (gas release from peatland) or decrease (gas uptake by peatland) in gas mass in the chamber. This fitting was done using the LINEST function in Excel.
f. Assuming the gradient is significant (positive or negative), calculate the *mass flux* density (F_g) of the gas.

The above procedure can be applied to small sets of data (i.e., those associated with syringe samples or a manually-read IRGA – sections 1.2.2 and 1.2.3) and the much larger sets of data associated with the UGA (hundreds of high-frequency readings – section 1.2.4). Threshold r^2 and p values were used to accept or reject the regression model obtained following the procedure above, and, depending on how measurements of gas concentrations were made, an r^2 threshold of between 0.7 and 0.9 was used. The threshold p value was always 0.05. If the r^2 falls below the threshold, and/or the p value is above its threshold, it is often assumed that there were problems with the chamber test; the data are rejected and a flux is not calculated. A problem with this 'traditional' approach is that it will tend to bias flux estimates: fluxes close to zero will be rejected and the flux average from a site will be artificially high (i.e., it will not include lower-end fluxes). This problem occurs because, as flux approaches zero, the gradient $\frac{dg_m}{dt}$ also tends to zero and the fitted regression line will have a low r^2. It has a low r^2 because the errors in any measurements, which tend to be fixed (such errors do not differ according to the flux), become relatively more important than the sum of squares of the regression (also called the explained sum of squares) which tends to zero as the slope of the best-fit regression line tends to zero. To account for this possibility, some authors (e.g., Green and Baird, 2012) have added another criterion to the test procedure: if the regression test 'fails' but the total variation (maximum – minimum) in chamber gas concentration is less than a threshold defined using the error typical for the

instrument used to measure the gas, the flux is assumed to be zero and a value of zero is recorded. In this way, fluxes of zero are retained and time-averaged or time-integrated fluxes from a collar or site are not biased to higher values. This error threshold approach was used on SP1210. In addition, for the high-frequency data obtained from the UPA, we were often able to detect small (albeit noisy, and therefore low R^2) trends in flux data with a high significance (i.e. $p < 0.001$) due to the large number of determinations. In this case, unless there was clear evidence of non-linearity or other unexplained variation based on visual inspection of the data (see below) the calculated flux was retained.

1.4. Flux estimates and 'problem' tests

We developed a detailed protocol for situations where the regression approach could not, initially, be applied to the flux test data or where it might yield misleading results. The detailed protocol is not included here but is available as two separate documents: SP1202_Defra_CH4_flux_analysis_protocol_SO.pdf and SP1210_Defra_CH4_flux_protocol_v2.pdf. The core principle behind the protocol is that all flux estimates should be made in sight of the data. That is, although a regression line with a high r^2 value and low p value may be fitted to the data it should not be assumed that the calculated flux value is reliable; it is necessary for those calculating fluxes to check that, graphically as well as numerically (p, r^2), the regression looks sensible. Although the full protocol is not reproduced here, it is instructive to consider one example from it to illustrate where problems may occur. Figure 1.2 shows a fictitious CH_4 concentration data series created to show what is sometimes seen in the high-frequency data available from the UGA. A regression analysis could be applied to the entire data set from 1650 to 1950 s and yield a very low p value and very high r^2. However, closer inspection of the series shows why this would be inappropriate. The initial noisy data enclosed by the red dashed line indicates a disturbance effect – associated with chamber emplacement – that is commonly seen in real data sets. In the protocol it was recommended that such noisy data were not included in the flux calculations. The series after the period of noise (from ~1700 s) shows CH_4 concentrations increasing over time, but, after ~1760 s, the rate of increase falling with time. This decline in the rate of increase may be due to increasing chamber CH_4 concentrations causing reductions in the CH_4 concentration gradient between the peatland soil and the chamber atmosphere, in turn causing reductions in rates of diffusion. There may be other, natural, reasons, for the change in the rate of concentration increase. However, because a test-related artefact cannot be ruled out, the protocol recommends that only the first part of the post-disturbance time series is used to calculate the flux (i.e., that part of the series enclosed by the green dashed line).

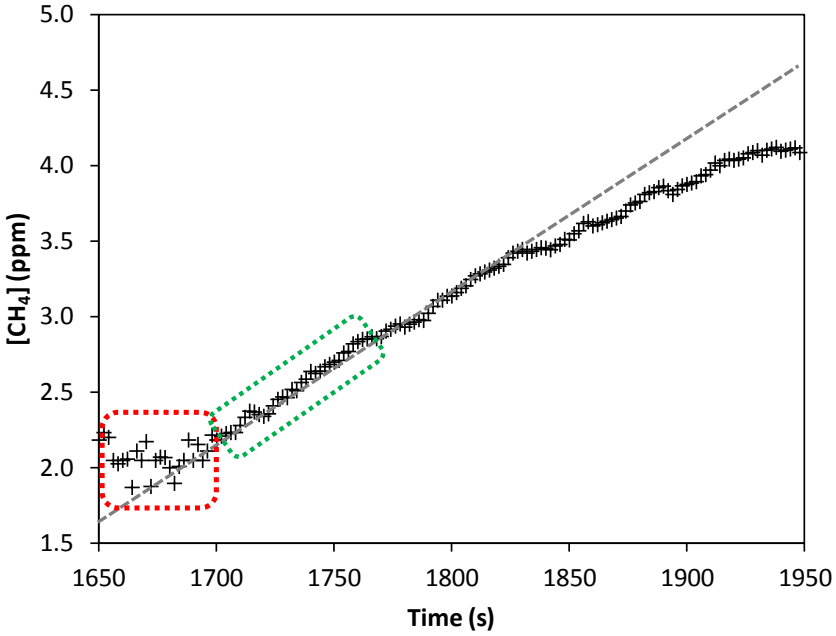

Figure 1.2. *A fictitious time series of within-chamber CH_4 concentrations showing three distinct components.*

1.5. Converting 'snapshot' flux estimates into time-integrated fluxes

Flux chamber measurements represent a snapshot in time and often will not represent conditions between measurements. For example, light flux chamber tests (i.e., those when the shroud is not in place) represent the balance between photosynthetic uptake of CO_2 by growing plants (gross primary productivity or *GPP*) and CO_2 production/release from the combination of plant and heterotrophic respiration (ecosystem respiration – *ER*). Plant uptake is very sensitive to solar irradiance which can vary minute by minute and hour by hour through the day as weather conditions change and the position of the sun in the sky varies. Other environmental factors can also affect fluxes such as air and soil temperature and water-table position, and these too may vary sufficiently between flux chamber tests to make simple interpolation between measurements unreliable when estimating carbon (C) budgets (budgets of CO_2 and CH_4) in particular. Therefore, to represent the periods between measurements accurately, it is necessary to develop models in which fluxes are related to a range of variables for which we have data for the intervening periods.

For each collar multiple flux measurements were made under a range of conditions, and these measurements were used to develop the models that could then be applied to the periods between measurements. A detailed protocol was written explaining how such models should be developed. The protocol was trialled with the site teams before being updated and implemented across the project. An edited version of that protocol is presented below.

1.5.1 Modelling gross primary productivity (GPP)

GPP is formally defined as:

$$GPP = NEE - ER \quad (3)$$

where *NEE* is net ecosystem CO_2 exchange (assumed negative here when there is net CO_2 uptake by the ecosystem) (M L^{-2} T^{-1} or mg CO_2 m^{-2} day^{-1}), and *ER* is ecosystem respiration (units as for *NEE*). *NEE* is what is

measured in a light chamber test and *ER* is what is measured in a dark chamber test. To model *GPP* on SP1210 the following equation or model was used:

$$GPP = \frac{Q \times I}{k + I} \times X_1 \times X_2 \times ... \times X_n \quad (4)$$

Q may be thought of as an asymptotic limit of *GPP* in the absence of other controlling factors (the *X*s – see below), *I* is irradiance(M T^{-3} W m^{-2}), and *k* is the so-called half saturation constant. This equation may be applied on a per collar basis or to groups of collars with similar vegetation. It produces a positive value for *GPP* which should be made negative for use in equation (3). Its two parameters that require fitting are *Q* and *k*. The fitting criterion that was used on SP1210 was the sum of the squared differences between observed values of *GPP* (calculated as the difference between the respective fluxes from a light chamber test and a dark chamber test) and the modelled values. Fitting was done using the Solver tool in Excel. The candidate multiplicative variables (X_1, X_2 etc) for the model were:

a. Air temperature
b. Soil temperature
c. Water-table depth
d. Temperature sum index
e. Abundance of different plant functional types (PFT) (more than one PFT could be considered in which case each one was treated as a separate multiplicative variable).

Air temperatures and, in many cases, soil temperatures were measured continuously (hourly) at each site by the automatic weather station (AWS). Water-table depth was, likewise, measured at high frequency in some wells, although not necessarily at the position of each collar.

The temperature sum index (*ETI*) has a daily resolution and is given by:

$$ETI_j = \left(\sum_{i=1}^{j} T_{air,i} \right) \Big/ j \quad (5)$$

where *j* is the day of interest counted from the first day when the five-day moving average air temperature exceeds a threshold temperature, T_{air} is daily-average air temperature (°C) and *i* is day number between 1 and *j*. The threshold temperature can be thought of as the temperature at which the vegetation of a site starts to grow and will differ across sites depending on the species make-up of the vegetation. To illustrate the use of equation (5) consider the 20th day since the beginning of the growing season. The average daily temperature of each of the first 20 days is summed (the numerator) and then divided by 20 to give the *ETI*. For the 21st day, the average daily temperature of each of the first 21 days is summed and then divided by 21 to give the *ETI*. The procedure continues until the five-day moving average air temperature falls below the threshold. For times of year for which the *ETI* is not calculated, *ETI* in the *GPP* model (equation (4)) may be set to 0 (in effect the *GPP* model is not applied) or to the threshold temperature value or to 1. The latter two may be used if it is thought that some photosynthesis occurs below the threshold temperature.

The *ETI* is a useful growing season variable that increases from spring to high summer before declining again later in the year. For some plant species, at least, it should track the rate at which plants grow and can, therefore, be a good predictor of *GPP*. However, it may co-vary with other variables such as air temperature and may not be retained in a model (because it won't add to the explanatory value of the variable with which it co-varies). Typically, ETI was found to be a useful explanatory variable for GPP where the plant species

present senesced during winter, but tended to over-predict seasonal variability (by effectively forcing GPP to zero during winter) for evergreen species.

PFT abundance was measured seasonally in the collars. If chamber data from several years are being used to produce the *GPP* model, the inclusion of PFT abundance data can be worthwhile, but much depends on how much the vegetation changes year-on-year.

Variables were only be retained in the final model if they made a 'worthwhile' difference to the fit of the model. There are many criteria that can be used to evaluate model fit. For SP1210 a regression line was fitted through the modelled *vs* measured data. The r^2 of the regression gives a measure of model fit to data, but can be biased when modelled *vs* measured deviates from a 1:1 line. It is possible, for example, for the model to show a consistent bias and the r^2 to be misleadingly high. One simple and easily understood remedy for this problem is to apply the following correction to the r^2 value which 'captures' how well the modelled *vs* measured values lie on the 1:1 line (Krause *et al*., 2005):

$$r_w^2 = a r^2,\ a \leq 1 \qquad (6a)$$

$$r_w^2 = r^2 / a,\ a > 1 \qquad (6b)$$

where r_w^2 is the weighted r^2 and a is the gradient of the regression line fitted to the modelled *vs* measured data.

Deciding on how many variables other than *I* to include in the model is not straightforward. Similarly, it is difficult to prescribe what value of r^2 or r_w^2 represents a satisfactory model fit. Model fitting is necessarily as much an art as it is a science. However, on SP1210 site teams were strongly advised to include variables in a model that added 0.05 or more to the value of r_w^2. In some cases the performance of the fitted models, as measured in terms of r_w^2, was fairly poor. In some cases this was (as for the individual flux determinations described in section 1.4) because all fluxes were fairly small, and leading to a low signal to noise ratio (although 'noise' in this case includes real variation that could not be explained by the suite of potential explanatory variables measured, rather than random errors alone). In most cases, we retained these models in the analyses, as they effectively provide a light-adjusted estimate of the mean rate of CO_2 uptake, which could not be obtained from a simple averaging of daytime measurements. Exceptions were made for intensively farmed sites, where seasonal variations in GPP were overwhelmingly controlled by farm operations (i.e. planting and harvesting) rather than meteorological conditions. At the two EF arable sites, eddy covariance data were used to obtain GPP. The treatment of chamber data from MM-DA and SL-IG is described in section 4.4. of the main report. The fitted GPP models for each site, and a number of model performance metrics, are given in Annex 1 of this appendix.

1.5.2 Modelling ecosystem respiration (ER)

ER is what is measured during a dark chamber test and was modelled on SP1210 using the following procedure. First, using the data from a single collar, or from a group of collars with similar vegetation, the measured *ER* values were plotted against their corresponding air temperatures. If the fit between the two approximated a straight line a regression line was fitted through the data. The bivariate regression model was extended to a multiple regression model by trying, in order, the following variables:

a. soil temperature
b. water-table depth
c. temperature sum index
d. PFT abundance.

As with the *GPP* model, variables were only retained in the final model if they made a difference of 0.05 or more to the value of r_w^2. The model produced through this process is a type of additive model of the form:

$$ER = a_1X_1 + a_2X_2 + ...+ a_nX_n + b \quad (7)$$

where the *X*s are explanatory variables. Model fitting was again done by minimising the sum of the squared differences between observed and predicted values (of, this time, *ER*) using the Solver tool in Excel, with the coefficients a_1, a_2 and so on being the fitting parameters. In producing the model it was sometimes found that soil temperature was a stronger predictor than air temperature. Because the two variables can be co-linear, air temperature was not always retained in the final model.

If the plot of *ER* against air temperature appeared to be non-linear, or if a satisfactory additive model could not be obtained, the following non-linear mixed multiplicative/additive model was used instead:

$$ER = \left[a_1 \times exp\left(a_2 T_{air}\right) \times ETI \times WT\right] + b \quad (8)$$

where a_1, a_2, and b are parameters to be fitted, T_{air} is now air temperature at the time of a flux test, *ETI* is temperature sum index and *WT* is water-table depth. Initially, data were fitted to a version of equation (8) without a_1, *ETI*, *WT* or b. The model was then extended by adding first a_1, then b, then *ETI*, and then *WT*. Because the term in brackets is multiplicative *ETI* was set to the threshold temperature for periods when actual temperatures were below the threshold. As with the *GPP* model, parameters (a_1, b) or variables (*ETI*, *WT*) were only retained if they made a difference of 0.05 or more to the value of r_w^2. Site teams were also encouraged to explore if PFT abundance could be included as a multiplicative term, like *ETI*, within the square brackets. They were also encouraged to explore whether a better model fit could be achieved by replacing T_{air} with T_{soil}. As for GPP, models performed worst where ER was low and relatively uniform over the year, for example at the extraction sites. In these cases, although r_w^2 was very low in some cases, the root mean squared error (RMSE) was also low, implying that the error in the estimated annual mean flux should also be small. Again, these models were retained, on the basis that even a poor-performing model should provide some improvement over a simple time-weighted mean. Fitted model parameters and performance metrics are given in Annex 1.

1.5.3 Modelling CH_4 flux

CH_4 fluxes were modelled in an identical way to *ER* with one major exception. In some graminoid species such as *Phragmites* CH_4 flux may be photosynthetically-driven. If such species occur in a collar, light-chamber test data (section 1.2.4) were used for fitting the model, with *I* included as a candidate variable in whichever model was being used (equation (7) or equation (8)). If equation (7) was the preferred model *I* was specified as the second candidate variable to try in the regression analysis. If the inclusion of *I* did not add substantially to the value of r_w^2 in a model in which T_{air} was already included, two bivariate models were compared, one with T_{air} as the sole candidate variable and one with *I*. The variable that produced the model with the higher r_w^2 was retained and then the other candidate variables tried according to the list shown above equation (7)

(so, from soil temperature onwards). If the additive model was unsatisfactory and a mixed model was used (equation (8)) *I* was tried as a candidate variable before *ETI* and *WT*. In many cases, no reliable model of CH_4 flux could be fitted to the observations based on the potential explanatory variables measured; in these cases, a simple time-weighted mean was used to estimate the annual flux.

2. Eddy covariance flux measurements and calculations

2.1 Eddy covariance

Eddy covariance (EC) is a micrometeorological technique that is widely used to measure turbulent flux densities (fluxes) of energy and mass across the interface between the land surface and the atmosphere (Baldocchi, 2003; 2014; Aubinet, Vesala & Papale, 2012). The EC technique is based on evaluating the mean covariance between the vertical motions of atmospheric turbulence and the concentrations of atmospheric scalars (Baldocchi, 2014). In contrast to chamber techniques, EC provides direct and (quasi-) continuous measurements of whole ecosystem flux dynamics without disturbing the ecosystem being studied (Baldocchi, 2003; 2014). The EC technique provides spatially-integrated flux measurements over a large source area (flux footprint) of tens to hundreds of meters upwind from the location of a flux tower (Rannik et al., 2012; Baldocchi, 2014).

The practical application of the EC technique employs fast response instrumentation (left panel Figure 2.1) installed on a flux tower above the canopy of an ecosystem (right panel in Figure 2.1). Sonic anemometer-thermometers are used to measure the horizontal (*u*; m s^{-1}), lateral (*v*; m s^{-1}) and vertical (*w*; m s^{-1}) components of atmospheric turbulence and the sonic temperature (T_s; ° C). Infrared gas analysers (IRGAs) are used to measure atmospheric concentrations of water vapour (g H_2O m^{-3}) and CO_2 (g CO_2 m^{-3}). More advanced gas analysers (e.g. quantum cascade lasers) are required for monitoring of other trace gas fluxes (e.g. CH_4, N_2O). Raw EC measurements are typically acquired at a rate of 10 to 20 Hz in order to capture the high frequency turbulent motion of the atmospheric boundary layer. Flux averaging intervals of 30 (to 60) minutes are typically used to calculate fluxes, reflecting a balance between requirements to capture low frequency atmospheric motions and the ability to resolve the diurnal pattern of mass and energy fluxes (Moncrief et al., 2004). Surface atmosphere flux densities (F_x) are computed as the mean covariance between instantaneous fluctuations in the vertical wind speed (w) and the atmospheric mixing ratio of the scalar of interest (x), using (after Foken, 2008):

$$F_x = \frac{1}{N-1}\sum_{i=0}^{N-1}[(w - \overline{w})(x - \overline{x})] \quad (9)$$

Where: overbars ($\overline{w}$,$\overline{x}$) denote time averages and N is the number of samples in a 30 minute flux averaging period (e.g. 36000 at a sampling rate of 20 Hz). IRGAs do not measure atmospheric mixing ratios of trace gases and fluxes must be adjusted for changes in air density related to variations in temperature and humidity (Webb, Pearman & Leuning, 1980).

***Figure 2.1**: Eddy covariance instrumentation at the Tadham Moor (SL-EG) site in Somerset. The left panel shows an R3-50 sonic anemometer (Gill Instruments ltd. Lymington, UK) and A LI7500 infrared H_2O/CO_2 analyser (LI-COR Biosciences Ltd., Lincoln, Nebraska, USA). The right panel shows the eddy covariance system installed over the vegetated canopy on 11th July 2014 (photographs: R. Morrison, Centre for Ecology and Hydrology).*

2.2 Eddy covariance instrumentation

Open-path EC systems were used at all SP1210 measurement sites (Table 2.1). Two types of sonic anemometer-thermometer were used across the network. CSAT3 sonic anemometers (Campbell Scientific Inc. Logan Utah, USA) were used at EF-EG, EF-DA and the two AF sites. R3-50 sonic anemometers (Gill Instruments, Lymington, UK) were deployed at the other three flux tower locations. All sites were equipped with either an LI-7500 IRGA (LI-COR Biosciences Ltd., Logan Utah, USA) or the more recent LI-7500A (LI-COR Biosciences Ltd., Logan Utah, USA). The measurement height at each location was set to at least two times the maximum canopy height (Table 2.1). During the project the measurement height was only changed at the EF-SA site in 2015, when it was necessary to raise it during a maize production cycle. EC systems were located to maximise the available fetch site from all wind sectors at each field. The exception was EF-DA, where the tower was positioned at the edge of a field to sample fluxes from a single land parcel located to the south west of the flux tower. The EC sensors were scanned at a rate of 20 Hz and logged using either LI-COR Biosciences LI7550 (at EF-LN, EF-EG) or Campbell Scientific CR3000 dataloggers (all other sites).

***Table 2.1**: Eddy covariance instrumentation installed at SP1210 eddy covariance sites*

Site	Sonic anemometer	Infrared gas analyser	Datalogger	Measurement height (m)
EF-LN	R3-50 [g]	LI7500A [l]	LI7550 [l]	3.9
EF-EG	CSAT3 [c]	LI7500A [l]	LI7550 [l]	2.4
EF-DA	CSAT3 [c]	LI7500 [l]	CR3000 [c]	1.6
EF-SA	R3-50 [g]	LI7500 [l]	CR3000 [c]	2.6 to 5 (for maize)
AF-LN	CSAT3 [c]	LI7500 [l]	CR3000 [c]	2.5
AF-HN	CSAT3 [c]	LI7500 [l]	CR3000 [c]	3.4
SL-EG	R3-50 [g]	LI7500 [l]	CR3000 [c]	2.8

***Notes**: Instrument manufacturers are denoted by subscripts: g, c and l refer to Gill Instruments Ltd. Lymington, UK; Campbell Scientific Inc., Logan, Utah, USA; and LI-COR Biosciences Ltd., Lincoln, Nebraska, USA, respectively.*

2.3 Ancillary instrumentation

A range of meteorological, energy balance and soil physics sensors were installed at each EC measurement sites (Table 2.2).

***Table 2.2**: Ancillary meteorological and soil physics instrumentation installed at SP1210 eddy covariance sites*

Site	R_{net}	SHF	T_{air}/RH	T_{soil}	VWC	Precip
EF-LN	CNR1 [k]	2 x HFP01 [h]	HMP45 [v]	TCAV [c]	2 x CS616 [c]	ARG10
EF-EG	CNR1 [k]	3 x HFP01-SC [h]	HMP45 [v]	TCAV [c]	3 x CS616 [c]	ARG10
EF-DA	CNR4 [k]	3 x HFP01-SC [h]	HMP45 [v]	TCAV [c]	3 x CS616 [c]	ARG10
EF-SA	CNR1 [k]	2 x HFP01 [h]	HMP45 [v]	PT07 [c]	2 xCS616 [c]	ARG10
AF-LN	NR-lite [k]	2 x HFP01 [h]	HMP45 [v]	TCAV [c]	2 x CS616 [c]	ARG10
AF-HN	NR-lite [k]	1 x HFP01 [h]	HMP45 [v]	PT07 [c]	1 x CS616 [c]	ARG10
SL-EG	CNR1 [k]	2 x HFP01 [h]	HMP45 [v]	PT07 [c]	2 x CS616 [c]	ARG10

***Notes**: R_{net} is the net radiation (W m^{-2}); SHF is soil heat flux (W m^{-2}); T_{air} is air temperature (° C); RH is relative humidity (%); T_{soil} is soil temperature (° C); VWC is volumetric soil water content (%); and Precip is precipitation (mm 30 $minutes^{-1}$). Instrument manufacturers are denoted by subscripts: k, h v and c refer to Kipp & Zonen, Delft, The Netherlands; Hukesflux Thermal Sensors B.V., Delft, The Netherlands; Vaisala, Helsinki, Finland; and Campbell Scientific Inc., Logan, Utah, USA, respectively.*

At most sites (excluding the two AF sites), the net radiation and its four components (incoming and outgoing short- and longwave radiation) were measured using four channel net radiometers. CNR1 net radiometers (Kipp & Zonen, Delft, The Netherlands) were installed at the majority of sites. A CNR4 net radiometer was installed at EF-DA (Kipp & Zonen, Delft, The Netherlands). Single channel NR-lite radiometers (Kipp & Zonen, Delft, The Netherlands) were installed at the AF-HN and AF-HN sites in combination with upward facing (shortwave) pyranometers (Didcot Instruments Ltd., Didcot, UK). HFP01 or HFP01-SC self-calibrating heat flux plates (Hukseflux Thermal Sensors B.V., Delft, The Netherlands) were installed below the soil surface to monitor the flux of heat into and out of the soil. Air temperature and relative humidity were measured using HMP45 (Vaisala, Helsinki, Finland) probes at all sites. Soil temperatures were monitored at most locations using either Campbell Scientific Inc. (Logan, Utah, USA) TCAV averaging thermocouples (at AF-LN, EF-DA, EF-

EG) or PT107 soil thermocouples (at EF-SA, SL-EG). Volumetric soil moisture content was measured at the majority of sites using CS616 time domain reflectometers (Campbell Scientific Inc., Logan Utah, USA). Precipitation was monitored using tipping bucket rain gauges (0.2 mm per tip).

2.4 Flux calculations

Thirty minute flux densities (fluxes) of sensible and latent heat (H and LE, respectively) and net ecosystem CO_2 exchange (NEE) were computed from the high frequency (20 Hz) measurements recorded by the sonic anemometers and IRGAs using EddyPRO Flux Calculation Software® version 6.0 (LI-COR Biosciences, Lincoln, Nebraska, USA). The EddyPRO flux calculation routine included:

- Removal of spikes and physically implausible values from the raw time series' (Vickers & Mahrt, 1997; Mauder et al., 2013);
- The angle of attack correction for Gill Instruments Ltd. sonic anemometers (Nakai et al., 2006). This correction was not applied to Campbell Scientific Inc. CSAT3 sonic anemometers.
- Dual-axis coordinate rotation to account the tilt of sonic anemometers relative to the local terrain (Wilczak et al., 2001);
- A covariance maximization procedure to remove time lags between the vertical wind speed and scalar signals;
- Calculation of mean covariances (uncorrected fluxes) as block averages over thirty minute flux averaging intervals (Moncrieff et al., 2004);
- Correction of fluxes for high (Moncrieff et al., 1997) and low frequency (Moncrieff et al., 2004) spectral attenuation;
- Correction of sensible heat fluxes for humidity effects (Schotanus et al., 1983);
- Adjustment of latent heat and then CO_2 fluxes for changes in air density related to humidity and temperature variation (Webb, Pearman & Leuning, 1980);
- Calculation of QC flags for each flux density (Foken & Wichura, 1996; Foken et al., 2004);
- Estimation of the flux footprint for each half hour period using the Kormann & Meixner (2001) analytical footprint model;
- Estimation of random flux uncertainties relating to sampling error (Finkelstein & Sims, 2001).

EC measurements are presented using the micrometeorological sign convention, where positive values indicate a flux from the surface to the atmosphere and negative values denote the reverse.

2.5 Quality control

A number of quality control (QC) procedures were applied to ensure that only high quality fluxes were retained for analysis.

- Statistical outliers were removed using the median absolute deviation method (Papale et al., 2006).

- Flux data of poor technical quality (inadequate turbulence and/or non-stationary measurement conditions) were removed on the basis of a 0 (high quality), 1 (acceptable quality), 2 (poor quality) quality flag system (Foken & Wichura, 1996; Foken et al., 2004). Data with a quality flag greater than 1 were excluded from further analysis.

- Fluxes were excluded when the nocturnal friction velocity was less than 0.1 m s^{-1}.

- Fluxes were removed between the ranges of -300 W m^{-2} to 500 W m^{-2} for H, -100 to 600 W m^{-2} for LE, and between 30 to -60 µmol CO_2 m^{-2} s^{-1} for NEE (and 30 to -65 µmol CO_2 m^{-2} s^{-1} for wheat and maize at EF-SA).

- Negative CO_2 flux densities were removed during nocturnal periods (incoming SW radiation less than 20 W m^{-2}).

- An analytical footprint model (Kormann & Meixner, 2001) was used to assess the spatial representativeness of the measured fluxes for each 30 minute period. Fluxes were retained for analysis when the results of the footprint model indicated 70% of the measured flux originated from the target land surface.

2.6 Data gap-filling

Gaps in EC flux datasets are unavoidable due to system failures and the removal of data during the application of quality control procedures (see above). A gap-filling method is required order to obtain daily and longer-term CO_2 and H_2O budgets (Moffat et al., 2007; Papale, 2012). Gaps in the EC datasets (H, LE, NEE) were filled using marginal distribution sampling (MDS; Reichstein et al., 2005; Reichstein et al., 2015). MDS is similar to mean diurnal variation (e.g. Falge et al., 2001) but improved to account for the temporal autocorrelation of fluxes and the covariance of fluxes meteorological drivers (Reichstein et al., 2005). In brief, the MDS approach fills data gaps using the mean of values obtained under similar micrometeorological conditions. Similar environmental conditions are defined as when incoming short wave radiation, air temperature and atmospheric vapour pressure deficit are within 50 W m^{-2}, 2 °C and 5 hPa of the values measured during each data gap, respectively. The size of the window used depends on the availability of data within the time period surrounding each data gap. The algorithm starts using a window size of seven days, subsequently increasing by an additional seven days if gap-filling is not possible within that window. The algorithm preform best when full time series of the key meteorological variables are available. If air temperature and VPD are unavailable, the algorithm is based on incoming shortwave radiation alone. In the case where incoming shortwave radiation is missing, data gaps are filled using the mean diurnal variation approach (Falge et al., 2001). In this study, priority was given to filling the prognostic meteorological variables prior to filling of fluxes in order to maximise the performance of the MDS algorithm. Gap-filling of flux datasets was performed using the REddyProc package (Reichstein et al., 2016) for the R Statistical Language (R Core Team, 2015).

2.7 Partitioning of net ecosystem CO_2 exchange

The net ecosystem exchange of CO_2 is the balance between two large fluxes: the release of CO_2 during auto- and heterotrophic respiration (termed total ecosystem respiration, TER) and the uptake of CO_2 during the photosynthesis of plants (gross primary production, GPP). GPP and TER were estimated from NEE using the approach of Reichstein et al. (2005) as implemented using the REddyProc Package (Reichstein et al., 2016) for the R statistical language (R Core Team, 2015). In this method, measured nocturnal CO_2 flux data (when

photosynthesis in inactive) are used to parameterise the exponential Lloyd & Taylor (1994) as a function of air temperature, as:

$$TER\ (T_{air}) = R_{10} \exp\left[E_0 \left(\frac{1}{T_{ref} - T_0} - \frac{1}{T_{air} - T_0}\right)\right] \quad (10)$$

Where: R_{10} is the basal respiration rate at a reference temperature (T_{ref}) of 10 °C; E_0 is an activation (temperature sensitivity) parameter; and T_0 is the temperature where TER is zero (set to -46.02 ° C to avoid the over parameterisation of the model). The E_0 parameter is fitted to the dataset, whereas R_{10} is fitted over shorter periods to better represent how the basal respiration rate changes with other time varying ecosystem properties (e.g. soil moisture, phenology). The parameterised function is used to estimate daytime TER. GPP is subsequently estimated as the difference between daytime measurements of NEE and the modelled TER, using:

GPP = |NEE-ER| (11)

2.8 Carbon dioxide and water budgets and uncertainties

CO_2 and water budgets were derived from the thirty minute flux data. Daily integrations of GPP, TER and NEE and ET were computed as the sum of the (measured and gap-filled) 48 thirty minute data points collected on each day (commencing after midnight). Longer-term (e.g. annual) integrals were calculated as the sum of the daily values. Uncertainties for thirty minute measurements of NEE and ET were estimated as the standard deviation derived from sampling errors (Finkelstein & Sims, 2001). For gap-filled data, uncertainties were estimated as the standard deviation of the values that were averaged to fill each missing data point (Reichstein et al., 2016). Daily and annual uncertainties were estimated as the sum of squares of the thirty minute uncertainties for each daily and annual period.

2.9 References

Aubinet, M., Vesala, T. & Papale, D. (2012). *Eddy Covariance: A Practical Guide to Measurement and Data Analysis*. Springer, Dordrecht.

Baldocchi, D. D. (2003). Assessing the eddy covariance technique for evaluating ecosystem carbon dioxide exchange rates of ecosystems: past present and future, *Global Change Biology.* **9**: 479-492.

Baldocchi, D., (2014). Measuring fluxes of trace gases and energy between ecosystems and the atmosphere – the state and future of the eddy covariance method, *Global Change Biology.* **20**: 3600-3609.

Denmead, O.T. (2008). Approaches to measuring fluxes of methane and nitrous oxide between landscapes and the atmosphere. *Plant and Soil*, **309**: 5-24.

Falge, E., Baldocchi, D., Olson, R., Anthoni, P., Aubinet, M., Berhhofer, C., Burba, G., Culemans, R., Clement, R., Dolman, H., Granier, A., Gross, P., Grünwald, T., Hollinger, D., Jensen, N., Katul, G., Keronen, P., Kowalski, A., Ta Lai, C., Law, B. E., Meyers, T., Moncrieff, J., Moors, E., Munger, J. W., Pilegaard, K., Rannik, Ü., Rebmann, C., Suyker, A., Tenhunen, J., Tu, K., Verma, S., Vesala, T., Wilson, K. & Wofsy, S. (2001). Gap filling strategies for defensible annual sums of net ecosystem exchange. *Agricultural and Forest Meteorology.* **107**: 43-69.

Finkelstein, P. L. & Sims, P. F. (2001). Sampling error in eddy correlation flux measurements. *Journal of Geophysical Research*, **106**: 3503-3509.

Foken, T. & Wichura, B. (1996). Tools for quality assessment of surface-based flux measurements. *Agricultural and Forest Meteorology.* **78**: 83-105.

Foken, T. (2008). *Micrometeorology*. Springer-Verlag Berlin Heidelberg.

Foken, T., Göckede, M., Mauder, M., Mahrt, L., Amiro, B. & Munger, W. (2004). Post Field Data Quality Control. In: *Handbook of Micrometeorology: A guide for surface flux measurement and analysis*, eds. X. Lee, W. Massman & B. Law, Kluwer Academic Press, Dordrecht, pp. 181-208.

Green, S.M and Baird, A.J. (2012). A mesocosm study of the role of the sedge *Eriophorum angustifolium* in the efflux of methane – including that due to episodic ebullition – from peatlands. *Plant and Soil*, **351**: 207-218.

Kormann, R. & Meixner, F. Z. (2001). An analytical footprint model for non-neutral stratification. *Boundary-Layer Meteorology.* **99**: 207-224.

Krause, P., Boyle, D.P., & Bäse, F (2005). Comparison of different efficiency criteria for hydrological model assessment. *Advances in Geosciences* **5**: 89-97.

Lloyd, J. & Taylor, J. A. (1994). On the temperature dependence of soil respiration. *Functional Ecology.* **8**: 315-323.

Mauder, M., Cuntz, M., Drüe, C., Graf, A., Rebmann, C., Schmid, H.P., Schmidt, M., Steinbrecher, R. 2013. A strategy for quality and uncertainty assessment of long-term eddy-covariance measurements, *Agricultural and Forest Meteorology*, **169**: 122-135.

Moffat, A. M., Papale, D., Reichstein, M., Hollinger, D. Y., Richardson, A. D., Barr, A. G., Beckstein, C., Brasswell, B. H., Churkina, G., Desai, A.R., Falge, E., Gove, J. H., Heimann, M., Hui, D., Jarvis, A. J., Kattage, J., Noormets, A. & Stauch, V. J. (2007). Comprehensive comparison of gap filling techniques for eddy covariance net carbon fluxes, *Agricultural and Forest Meteorology.* **147**: 209-232.

Moncrieff, J. B., J. M. Massheder, H. de Bruin, J. Ebers, T. Friborg, B. Heusinkveld, P. Kabat, S. Scott, H. Soegaard, and A. Verhoef. 1997. A system to measure surface fluxes of momentum, sensible heat, water vapor and carbon dioxide. *Journal of Hydrology*, 188: 589-611.

Moncrieff, J., Clement, R., Finnigan, J. & Meyers, T. (2004). Averaging, detrending, and filtering of eddy covariance time series. In: *Handbook of Micrometeorology*, eds. X. Lee, W. Massman & W. Law, Kluwer Academic Press, Dordrecht, pp. 7-31.

Nakai, T., M. K. van der Molen, J. H. C. Gash, and Y. Kodama. 2006. Correction of sonic anemometer angle of attack errors. Agricultural and Forest Meteorology, 136: 19-30.

Papale, D., Data Gap Filling In: M. Aubinet et al. (Eds.), *Eddy Covariance: A Practical Guide to Measurement and Data Analysis*, Springer, Dordrecht, 159-172

Papale, D., Reichstein, M., Aubinet, M., Canfora, E., Bernhofer, C., Kutsch, W., Longdoz, B., Rambal, S., Valentini, R., Vesala, T. & Yakir, D. (2006). Towards a standardized processing of Net Ecosystem Exchange measured with the eddy covariance technique: algorithms and uncertainty estimation. *Biogeosciences.* **3**:571-583.

R Core Team, (2016). *R: A Language and Environment for Statistical Computing*. R Foundation for Statistical Computing, Vienna, Austria. https://www.R-project.org/

Rannik, Ü., Sogatchev, A., Foken, T., Göckede, M., Kljun, N., Leclerc, M. Y. & Vesala, T. Footprint analysis, In: M. Aubinet et al. (Eds.), *Eddy Covariance: A Practical Guide to Measurement and Data Analysis*, Springer, Dordrecht, 211-261

Reichstein, M. Falge, E., Baldocchi, D., Papale, D., Aubinet, M., Berbigier, P., Bernhofer, C., Buchmann, N., Gilmanov, T., Granier, A., Grünwald, T., Havránkova, K., Ilvesniemi, H., Janous, D., Knohl, A., Laurila, T., Lohila, A., Loustau, D., Matteucci, G., Meyers, T., Miglietta, F., Ourcival, J.-M., Pumpanen, J., Rambal, S., Rotenberg, E., Sanz, M., Tenhunen, J., Seufert, G., Vaccari, F., Vesala, T., Yakir, D. & Valentini, R. (2005a). On the separation of net ecosystem exchange into assimilation and ecosystem respiration: review and improved algorithm. *Global Change Biology*. **11**, 1424-1439. Reichstein et al., 2015

Reichstein, M., Moffat, A. M., Wutzler, T. & Sickel, K. (2016*). REddyProc: Data processing and plotting utilities of (half-)hourly eddy-covariance measurements*. R package version 0.8-2/r14 https://R-Forge.R-project.org/projects/reddyproc/

Reichstein, M., Stoy, P. C., Desai, A. R., Lasslop, G. & Richardson, A. D. Partitioning of net fluxes. In: M. Aubinet et al. (Eds.), *Eddy Covariance: A Practical Guide to Measurement and Data Analysis*, Springer, Dordrecht, 211-261

Schotanus, P., Nieuwstadt, F. T. M. & Bruin, H. A. R. (1983). Temperature measurement with a sonic anemometer and its application to heat and moisture fluxes. *Boundary Layer Meteorology.* **26**: 81-93.

Vickers, D. & Mahrt, L. (1997). Quality Control and Flux Sampling Problems for Tower and Aircraft Data. Journal of Atmospheric and Oceanic Technology. 14: 512-526.

Webb, E. K., Pearman, G. I. & Leuning, R. (1980). Correction of flux measurements for density effects due to heat and water vapour transfer. *Royal Meteorological Society Quarterly Journal.* **106**: 85-100.

Wilczak, J. M., Oncley, S. P. & Stage, S. A. (2001). Sonic anemometer tilt correction algorithms. *Boundary-Layer Meteorology.* **99**: 127-150.

ANNEX 1. FITTED STATIC CHAMBER FLUX MODELS

Models of Gross Primary Production (GPP)

The following table shows the explanatory variables, parameter values and model performance metrics for GPP (for explanation of terms see preceding text. Note that, although all GPP models follow a fundamentally similar form, the exact terms used vary slightly between sites. Note that GPP was not modelled for intensive agricultural or extraction sites. Chamber fluxes at the Norfolk Broad sites were modelled separately as part of a PhD studentship, prior to the development of project-wide analysis protocols and based on a different set of evaluation metrics. The resulting models are therefore shown in a separate table below.

Site and vegetation type	**Equation**	**Parameters Used**	**GP max**	**Alpha**	**a**	**b**	**R^2**	**Weighted R^2**	**RMSE**
MM-RW (*Molinia* dominated)	$GPP = \frac{GPmax * \propto * PAR}{GPmax + (\propto * PAR)} * (a * airtemp) + (b * WT)$	PAR Air temperature Water table depth	0.033	398.8	1653.2	-0.449	0.186	0.043	563
MM-RW (*Sphagnum* dominated)	$GPP = \frac{GPmax * \propto * PAR}{GPmax + (\propto * PAR)} * (a * airtemp) + (b * WT)$	PAR Air temperature WT	0.015	398.8	758.8	-2.031	0.042	0.002	215
MM-RW (*Molinia* & *Eriophorum*)	$GPP = \frac{GPmax * \propto * PAR}{GPmax + (\propto * PAR)} * (a * airtemp) + (b * WT)$	PAR Air temperature WT	0.019	398.7	951.5	-0.743	0.108	0.01	330
		Parameters Used	**Q**	**k**	**a**	**b**	**R^2**	**Weighted R^2**	**RMSE**
EF-EG Juncus	$GPP = \frac{(Q * PAR)}{k + PAR} * airtemp$	PAR Air temperature	87.39	45.62			0.113	0.019	1152
EF-EG Agrostis	$GPP = \frac{(Q * PAR)}{k + PAR} * airtemp$	PAR Air temperature	97.50	0.01			0.173	0.034	1203
EF-LN	$GPP = \frac{(Q * PAR)}{k + PAR} * airtemp * WT$	PAR	1662900	12291000			0.239	0.086	920

Cladium		Air temperature WT							
EF-LN Phragmites	$GPP = \frac{(Q * PAR)}{k + PAR} * airtemp * WT$	PAR Air temperature WT	14608000	96830000			0.332	0.124	892
SL-IG (all)	$GPP = \frac{(Q * PAR)}{k + PAR} * airtemp$	PAR Air temperature	184	246			0.46	0.236	864
SL-EG (all)	$GPP = \frac{(Q * PAR)}{k + PAR} * airtemp$	PAR Air temperature	140	217			0.241	0.082	913

Models of Ecosystem Respiration (ER)

	Equation	Parameters Used	a	b	R^2	Weighted R^2	RMSE
EF-EG Juncus	$Reco = b * e^{a*airtemp}$	Air temperature	0.050	187.9	0.090	0.008	507
EF-EG Agrostis	$Reco = b * e^{a*airtemp}$	Air temperature	0.057	254.9	0.129	0.014	673
EF-LN Cladium	$Reco = b * e^{(a*airtemp)*WT}$	Air temperature WT	0.045	98.3	0.235	0.039	205
EF-LN Phragmites	$Reco = b * e^{(a*airtemp)*WT}$	Air temperature WT	0.089	62.7	0.452	0.177	274
MM-RW (*Molinia* dominated)	$Reco = b * e^{a*airtemp}$	Air temperature	0.0693	169.0	0.255	0.072	334
MM-RW (*Sphagnum* dominated)	$Reco = b * e^{a*airtemp}$	Air temperature	0.0729	55.0	0.323	0.11	121
MM-RW (*Molinia* & *Eriophorum*)	$Reco = b * e^{a*airtemp}$	Air temperature	0.0754	98.1	0.33	0.108	234
MM-DA (all)	$Reco = b * e^{a*airtemp}$	Air temperature	0.1434	81.2		0.119	936
MM-EX (all)	$Reco = b * e^{a*airtemp}$	Air temperature	0.0253	37.1	0.0133	0.0003	47.6
SL-IG (all)	$Reco = b * e^{a*soiltemp}$	Soil temperature at 10 cm	0.122	214.0	0.594	0.356	493
SL-EG (all)	$Reco = b * e^{a*soiltemp}$	Soil temperature at 30 cm	0.130	164.0	0.419	0.17	469

Equations used to model GPP, ER and CH_4 fluxes at the Norfolk Broad sites

	Equation	-loglik	-loglik df	AICc w_i	NSE	Notes
VGA	$Daily\ VGA = VGA_{max} \cdot e^{(-0.5\left(\frac{julian - x_{max}}{b}\right)^2)}$	302	16	N/A	0.71	VGA infill model created using mixed-effects non-linear least square regression, where $Daily\ VGA$ ($m^2\ m^{-2}$) is the response variable; $julian$ is the day-of-year number, an independent variable (no site fixed effect); VGA_{max} ($m^2\ m^{-2}$), x_{max} and b are fitted parameters; and random variation between collars for fitted parameters.
ER	$ER = (\mathrm{Rx} + \mathrm{b1} \cdot \mathrm{VGA}) \cdot \exp(\mathrm{b2} \cdot \mathrm{PT}) \cdot \exp(\mathrm{b3} \cdot \mathrm{WL})$	1042	6	0.57	0.66	Reco modelled using non-linear mixed-effects approach. Basal ecosystem respiration at 0 °C (Rx; mg $CO_2\ m^{-2}\ h^{-1}$), VGA ($m^2\ m^{-2}$), peat temperature at 5 cm (PT; ˚C) and water level (WL; cm above peat surface) are the independent variable (no site fixed effect) and the model has the same slope for both sites but with random variation (intercept) between collars.
GPP	$GPP = pmax \cdot (\frac{par}{kpar + par}) \cdot VGA^{(kabs \cdot \exp(ktemp \cdot AT) \cdot \exp(kwl \cdot WL))}$	1080	8	0.59	0.69	GPP modelled using non-linear mixed-effects approach. PAR (µmol $m^{-2}\ s^{-1}$), Vascular Green Area ($m^2\ m^{-2}$), air temperature (AT; ˚C) and water level (WL; cm above peat surface) are the independent variable (no site fixed effect) and random variation between collar for pmax (mg $CO_2\ m^{-2}\ h^{-1}$). Kpar (µmol $m^{-2}\ s^{-1}$), kabs, ktemp and kwl are fitted parameters.
CH_4	$logCH4 = a \cdot ZPT2 + b \cdot ZBaro + c \cdot ZBaro2 + (1\|Site)$	83.1	6	0.19	0.62	CH_4 modelled using linear mixed-effects approach. ZPT2 (standardised peat temperature squared), ZBaro (Standardised barometric pressure), ZBaro2 (ZBaro squared) and ZWS (standardised wind speed$^{0.6}$) are the independent variable (no site fixed effect) and the model has the same slope for both sites but with random variation (intercept) between collars.
NSE	$NSE = 1 - \frac{\sum_{i=1}^{n}(O_i - P_i)^2}{\sum_{i=1}^{n}(O_i - \bar{O})^2}$					NSE coefficient used to compare observed and predicted data (the range in E lies between 1.0, a perfect fit, and $-\infty$); O is observed and P is predicted values.

-loglik and -loglik df are measured of goodness of fit; AICc = corrected Akaike Information Criterion, which allows inter-model comparison